






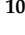



Article

Modeling and Optimization of Energy and Exergy Parameters of a Hybrid-Solar Dryer for Basil Leaf Drying Using RSM

Zahra Parhizi ¹, Hamed Karami ² , Iman Golpour ³ , Mohammad Kaveh ^{4,*} , Mariusz Szymanek ^{5,*} , Ana M. Blanco-Marigorta ⁶ , José Daniel Marcos ⁷ , Esmail Khalife ⁸ , Stanisław Skowron ⁹, Nashwan Adnan Othman ¹⁰  and Yousef Darvishi ¹¹ 

- ¹ Chemical Engineering Department, Amirkabir University of Technology, Tehran 15875-4413, Iran; zparhizi@aut.ac.ir
 - ² Department of Biosystems Engineering, University of Mohaghegh Ardabili, Ardabil 56199-11367, Iran; hamedkarami@uma.ac.ir
 - ³ Department of Mechanical Engineering of Biosystems, Urmia University, Urmia 57561-51818, Iran; imangolpour@gmail.com
 - ⁴ Department of Petroleum Engineering, College of Engineering, Knowledge University, Erbil 44001, Iraq
 - ⁵ Department of Agricultural, Forest and Transport Machinery, University of Life Sciences in Lublin, 20-612 Lublin, Poland
 - ⁶ Department of Process Engineering, Universidad de Las Palmas de Gran Canaria, 35017 Las Palmas de Gran Canaria, Spain; anamaria.blanco@ulpgc.es
 - ⁷ Department of Energy Engineering, Universidad Nacional de Educación a Distancia, UNED, 28040 Madrid, Spain; jdmarcos@ind.uned.es
 - ⁸ Department of Civil Engineering, Cihan University-Erbil, Kurdistan Region, Erbil 44001, Iraq; esmail.khalife@su.edu.krd
 - ⁹ Department of Strategy and Business Planning, Faculty of Management, Lublin University of Technology, 20-618 Lublin, Poland; s.skowron@pollub.pl
 - ¹⁰ Department of Computer Engineering, College of Engineering, Knowledge University, Erbil 44001, Iraq; nashwan.othman@knu.edu.iq
 - ¹¹ Department of Biosystems Engineering, University of Tehran, Tehran 11365-4117, Iran; sdarvishi@ut.ac.ir
- * Correspondence: sirwan.kaweh@knu.edu.iq (M.K.); mariusz.szymanek@up.lublin.pl (M.S.)



check for updates

Citation: Parhizi, Z.; Karami, H.; Golpour, I.; Kaveh, M.; Szymanek, M.; Blanco-Marigorta, A.M.; Marcos, J.D.; Khalife, E.; Skowron, S.; Adnan Othman, N.; et al. Modeling and Optimization of Energy and Exergy Parameters of a Hybrid-Solar Dryer for Basil Leaf Drying Using RSM. *Sustainability* **2022**, *14*, 8839. <https://doi.org/10.3390/su14148839>

Academic Editor: Akbar Maleki

Received: 10 June 2022

Accepted: 16 July 2022

Published: 19 July 2022

Publisher's Note: MDPI stays neutral with regard to jurisdictional claims in published maps and institutional affiliations.



Copyright: © 2022 by the authors. Licensee MDPI, Basel, Switzerland. This article is an open access article distributed under the terms and conditions of the Creative Commons Attribution (CC BY) license (<https://creativecommons.org/licenses/by/4.0/>).

Highlights:

- An exergy and energy analysis during basil leaf drying is performed.
- Factors investigated include drying rate, energy utilization, energy utilization ratio, exergy efficiency, exergy loss, improvement potential rate, and sustainability index.
- Exergy efficiency varied in the range of 31.78–86.55%.
- The optimal conditions for basil drying were at an air temperature of 63.8 °C and a bed thickness of 2 cm.

Abstract: This study deals with the optimization of energetic and exergetic parameters of a hybrid-solar dryer to dry basil leaves under determined experimental conditions at three air temperatures (40 °C, 55 °C, and 70 °C) and three bed thickness levels (2, 4, and 6 cm). The optimization of the thermodynamic parameters was performed using the response surface method (RSM) based on the central composite design (CCD) and the desirability function (DF) to maximize the drying rate, exergy efficiency, improvement potential rate and the sustainability index, and to minimize the energy utilization, energy utilization ratio and exergy loss rate. These parameters were calculated on the basis of the first and second laws of thermodynamics as the response variables. Based on the results obtained, it was determined that the optimal conditions for basil drying were at a drying air temperature of 63.8 °C and a bed thickness of 2 cm. At this point, the parameters of the drying rate, energy utilization, energy utilization ratio, exergy efficiency, exergy loss rate, improvement potential rate and sustainability index were obtained with the maximum utility function ($D = 0.548$) as 0.27, 0.019 (kJ/s), 0.23, 65.75%, 0.016 (kJ/s), 1.10 (kJ/s) and 0.015, respectively.

Keywords: basil leaves; solar-forced convective dryer; energy and exergy evaluation; RSM; desirability function

1. Introduction

Basil (*Ocimum basilicum*) is one of the most important plants of the Lamiaceae family, is an annual herbaceous plant that grows to 20–60 cm in length and its flowers are a purple-white color. Basil originated in India and Iran and is cultivated in Mediterranean countries and regions with temperate, hot, and dry climates [1]. In addition to having a considerable commercial value, it can be applied in food preparation as a spice, a fresh vegetable, a medicinal plant, an antimicrobial, an antiviral, and as an antioxidant [2,3].

In the past, food preservation methods were very inexpensive and these may still be the best option for economically disadvantaged communities. Today, these methods are still utilized in special situations such as during famines, floods, earthquakes, and long-term power outages in natural environments; therefore, with the industrialization of societies, the growth of populations and their distribution throughout the world, specialized agriculture in certain geographic areas, and the prosperity of the global economy, the need for optimal food storage has been doubled to provide the best protection for assuring food quality from the farm during harvest, to transportation, distribution, and finally for utilization at the lowest cost. Since most drying processes are carried out at high temperatures, the quality characteristics of the dried product, such as its texture, nutritional value, taste, color, and aroma, are adversely affected. To minimize these changes, the drying methods and conditions such as temperature, drying time, air velocity, and so on, must be optimized [2].

The drying process is one of the most essential and common steps in the post-harvest processing of herbal plants such as basil and, therefore, it has a significant impact on the volatile components of the essential essence. Drying reduces the humidity of crops and is the most crucial procedure for safeguarding agricultural products because it has a considerable impact on the condition of parched goods [4]. In addition to extending the shelf life, drying herbal products can also diminish the activity of enzymes and microorganisms [5]. As agricultural products have a low thermal conductivity, heat is transferred slowly to their interior; therefore, their drying process consumes a significant amount of energy. Choosing a suitable drying method and shortening the drying time not only achieves economic savings but also reduces undesirable product changes, such as in texture, nutritional value, taste, color, and aroma [6]. Two traditional methods (e.g., spreading in the sun or shade) and industrial methods (e.g., a hot air-convective dryer with burner heating or electric heaters) are used to dry herbal plants. Generally, these methods have some limitations, such as requiring a long drying time, exposure to dust and rain, a high initial investment cost, high energy utilization (due to the use of fossil fuels), an accumulation of greenhouse gases in the atmosphere followed by global warming, and environmental pollution. Therefore, it seems necessary to dry herbal plants with a dryer that uses the radiant energy of the sun to shorten the drying time and improve the final quality of the dried plants. The utilization of a solar dryer is considered a new solution in this regard and is growing rapidly in popularity. This kind of dryer releases heated air from solar panels over the product and has an energy efficiency comparable to industrial dryers in areas with high solar radiation during the harvesting season. Hence, they can easily be substituted for traditional and industrial drying methods [7].

Drying represents one of the most extensive processes in energy usage, consuming between 12 and 25% of the total energy in industrial processing. About 30% of the world's total energy consumption is utilized by the agricultural sector, out of which 3.62% is used for drying agricultural products [8]. In the last decade, in the face of increasing energy utilization, both energy loss and exergy (the maximum work that can be performed with a given amount of available energy or with a material flow) have gained importance in thermodynamic research [9,10]. The main goal of exergy analysis is to determine the

location and amount of irreversibility during the different processes in the thermodynamics cycle and to identify the factors that influence this irreversibility. In this way, not only the efficiency of the various components of the thermodynamics cycle is evaluated, but also the opportunities of improving the overall efficiency of the cycle are identified. Golpour et al. [11] studied the energy and exergy loss of the potato drying process in a convection dryer and found that the exergy losses, exergy efficiency, and rate of improvement potential ranged from 0.006–0.0366 kJ/s and 57.07–85.85%, and 0.0016–0.0046 kJ/s, respectively. In another study, the thermodynamics evaluation of a fluidized bed dryer at different temperatures and bed heights for Kodo millet drying was investigated by Yogendrasidhar and Pydi Setty [12]. The results of this study showed that the exergy efficiency increased with an increasing temperature and bed height. Beigi et al. [13] also analyzed the energy and exergy performance of a semi-industrial dryer for drying paddy samples. According to the results of that study, the energy utilization and energy utilization ratio decreased while the exergy losses and exergy efficiency parameters increased with an increasing drying air velocity and air temperature.

The optimization of thermodynamics parameters is usually undertaken in the manufacturing industry, particularly with dryers, to improve the final product quality while reducing the energy utilization and maximizing the cost-efficiency; therefore, the analysis of the energy and exergy parameters is one of the most important techniques to optimize and improve the efficiency of a dryer [14]. The optimization of processes leads to energy savings through the development of new dryers and modifications to existing systems. Advanced exergy analysis is used to quantify and characterize the inefficiency of an energy system [15,16], and to evaluate the thermodynamics and economic performance of an energy system, its actual potential for improvement and its system parameters must be effectively considered [17].

Evaluating the optimal performance of the process parameters used in the food industry is a very important task because they directly affect the quality of the final product, production efficiency, energy efficiency, production costs, and the time to a product's delivery [14,18]. The response level method is a set of statistically specific techniques for building models, evaluating the effects of independent factors, and determining the optimal conditions for achieving desired outcomes. Box and Wilson first introduced the response-level method in 1951. The response-level method allows multicomponent experiments to be carried out simultaneously with a minimum experimental time, testing the most important factors and their interactions with each other [19]. It has been used to optimize the drying process of *Laurus Nobilis* [20], mint [21], pear wedges [22], tomatoes [23], lemons [24], and onions [25]. Sadeghi, Asl, and Movagharnejad [26] optimized the quality of kiwifruit slices in a convection infrared dryer using the response surface method with the independent variables of infrared power, kiwifruit slice thickness, the distance between kiwifruit slice and infrared lamps and air velocity, and the dependent variables of drying time, drying rate and shrinkage. Based on their research, all the independent variables had a significant effect on the dependent variables, but the kiwi slice thickness was the most significant. Majdi, Esfahani, and Mohebbi [27] studied how a convection dryer was optimized for drying apple slices by the response surface method with a maximum desirability function of 0.781. In the study of Jafari, Movagharnejad, and Sadeghi [28] the effects of an infrared drying process on eggplant slices were evaluated via the surface response technique using the Box–Behnken design (BBD). According to the results of that study, the optimal values for the eggplant slicing were 4.9 cm, air velocity of 1.14 m/s, and infrared power of 1500 W, while the optimal values for the responses of the TPC, ΔE , and Potassium concentrations were 2531.82 mgGA/100 gdm, 21.23 and 1929.85 mg/100 gdm, respectively. Using a hot air convection dryer with pretreatments, a study evaluated the energy, exergy, and sustainability index parameters for drying pumpkin seeds using the surface response method. The results showed that the optimal values for energy and exergy efficiency were 13.40% and 41.77%, respectively; therefore, the values for the sustainability index and improvement potential were related to the exergy losses [29]. In recent studies, the influence of the drying

air temperature and bed thickness drying conditions on changes in the energy and exergy parameters of the basil leaf drying process have not been investigated; hence, to optimize the drying process, the current research focused on modeling the influence of the air temperature bed thickness (as the independent variables) on changes in the moisture content, drying rate (DR), energy utilization, energy utilization ratio, exergy efficiency, exergy loss, improvement potential rate, and sustainability index (as the dependent variables) of a hybrid-solar drying process for basil leaves by using the RSM method.

2. Materials and Methods

2.1. Preparation of Sample

The basil plants used in the present study was purchased in the Miandarband region, Kermanshah. To preserve their freshness, it was washed and stored in a refrigerator at 4 ± 1 °C. As part of the daily test, they were removed from the refrigerator and cleaned (removing the superfluous parts such as unusable leaves and roots). To determine the initial moisture content of the basil, samples of 50 g were randomly taken out of the refrigerator, then the standard oven method was applied for 1 h at 105 °C [1]. Finally, the average initial moisture of the basil leaves obtained was $83.20 \pm 3\%$ (w.b.). The basil leaves drying experiments were performed in three replications.

2.2. Drying Equipment and Empirical Method

In this study, a hybrid-solar dryer (HSD) with manufactured hot air [30] was employed to dry the basil leaves in June 2021 as shown in Figure 1.

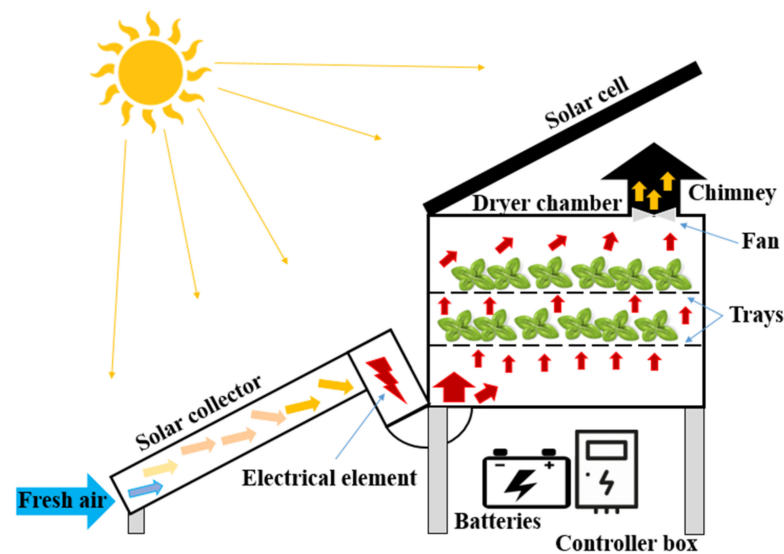


Figure 1. Schematic diagram of a laboratory hybrid-solar dryer with an automatic control system.

In addition to a control system to measure the air temperature, air velocity, and relative humidity, the dryer had a solar collector and a drying chamber with two aluminum perforated trays, in which the volume of the drying chamber was 210 cm³. In this type of dryer, the frame of the solar collector was made of aluminum and black aluminum sheets with air-conducting blades to absorb sunlight. The solar collector was inclined at 34° from the horizontal, with 1.20 m of length, 1 m of width, and 0.07 m of internal height. In addition, a 1000 W electric element heated the inlet air of the dryer chamber, which could be varied by a fan located inside the collector. To measure the velocity of the air entering the dryer chamber, an AVM-07 vane velocity meter made in Taiwan with a measurement accuracy of 0.1 m/s was used. There was also an air outlet at the top of the solar drying chamber to direct the air outside. Additionally, five LM75 sensors (Sigma-Delta, Ann Arbor, MI, USA) with a measurement accuracy of -55 °C to 125 °C (± 2 °C), and two

HS101 sensors (model HS1101, Apollo Electronics Co., Ltd., Guangdong, China) with a measurement accuracy of $\pm 2\%$ were applied to measure the air circulation temperature and relative humidity, respectively. During the experiments, the solar radiation that reached the absorber plate was in a range between 36–49 MJ/m², while the relative humidity and the temperature of the ambient air were $17 \pm 2\%$, and 30–35 °C, respectively. Moreover, the relative humidity of the air leaving the dryer was 55% at the beginning of the test and 15% at the end of the process.

The basil dryer was set for 30 min to reach a sustainable state before carrying out the drying experiments. The prepared samples were weighed with a digital scale (A&D model GF3000, Tokyo, Japan) in the value ranges of 200, 400, and 600 g, and then evenly distributed on the drying trays in the sizes of 2, 4, and 6 cm. They were dried at three different temperatures of 40 °C, 55 °C, and 70 °C, whereas a constant air velocity of 1 m/s was used for all the experiments. All the tests were performed in three replicates and all the samples were treated with the same drying conditions.

2.3. Data Analysis

2.3.1. Moisture Ratio and Drying Rate Analysis

Because of the reduction in data dispersion, the drying kinetics are often evaluated using two-parameter indicators of the moisture ratio and drying rate. In the present study, the moisture ratio and drying rate of the basil leaves were calculated using Equations (1) and (2) [30]:

$$MR = \frac{M_t - M_e}{M_o - M_e} \quad (1)$$

$$DR = \frac{M_t - M_{t+\Delta t}}{\Delta t} \quad (2)$$

Energy Utilization

The drying process of the basil was considered as a stable flow process in order to perform an energy analysis using the Equations (3)–(13). The energy balance of the input and output flows of the dryer was analyzed using Equation (5) as a general energy conversion equation. Equations (3) and (4) were used to calculate the air characteristics, i.e., the dry air density and the enthalpy of the dry air [31,32]. Additionally, Equation (5) was employed to calculate the energy utilization (EU):

$$\rho_a = \frac{101.325}{0.287(T_a + 273.16)} \quad (3)$$

$$h_a = c_a(T_a - T_\infty) + h_{fg}\omega \quad (4)$$

$$EU = \dot{m}_{ina} \cdot h_{ina} + \dot{m}_{fp} h_{fp} - \dot{m}_{outa} h_{outa} - \dot{m}_{dp} h_{dp} - \dot{Q}_L \quad (5)$$

Equation (6) was used to calculate the heat transfer rate within the dryer [33]:

$$\dot{Q}_{evp} = \dot{m}_{ina} h_{fg} \omega \quad (6)$$

Energy Utilization Ratio

The enthalpy of the fresh and dry products was calculated by first determining the specific heat of the input or output product. A GM900 laser thermometer was applied to measure the temperature parameters of the inlet and outlet of the product as well as the ambient temperature [34]:

$$h_b = c_p(T_b - T_\infty) \quad (7)$$

The following equation was also used to determine the specific heat capacity of the dryer inlet and outlet air [33–35]:

$$c_{pa} = 1.004 + 1.88\omega \quad (8)$$

The humidity rate was calculated using the following equation [34]:

$$\omega = 0.622 \frac{\varphi P_{vs,a}}{P - \varphi P_{vs,a}} \quad (9)$$

Finally, Equations (10)–(13) were utilized to calculate the rate of heat removed from the air leaving the dryer and the heat loss from the dryer body, as well as the energy utilization ratio (EUR) [31,33]:

$$\dot{Q}_{al} = \dot{m}_{ina} c_{pda} (T_{ina} - T_{outa}) \quad (10)$$

$$\dot{Q}_{hdb} = UA_{hdb} (T_{tp} - T_{\infty}) \quad (11)$$

$$U = \frac{\dot{m}_{ina} c_{pina} (T_{ina} - T_{outa})}{A_{hdb} (T_{tp} - T_{\infty})} \quad (12)$$

$$EUR = \frac{\dot{m}_{ina} h_{ina} + \dot{m}_{fp} h_{fp} - \dot{m}_{outa} h_{outa} - \dot{m}_{dp} h_{dp} - \dot{Q}_L}{\dot{m}_{ina} (h_{ina} - h_{\infty})} \quad (13)$$

Exergy Evaluation

In general, the exergy analysis was performed according to the first and second laws of thermodynamics, which was evaluated to obtain the specific exergy of air, exergy loss, and exergetic efficiency of the dryer chamber using Equations (14)–(16) [33,34]:

$$ex_{da} = C_{pda} (T - T_0) - T_0 \left[c_{pda} \ln \left(\frac{T}{T_0} \right) \right] + T_0 \left[R \ln \left(\frac{1 + 1.6078\omega_0}{1 + 1.6078\omega} \right) \right] + 1.6078\omega R \ln \left(\frac{\omega}{\omega_0} \right) \quad (14)$$

$$Ex_L = Ex_{in} - Ex_{out} \quad (15)$$

$$\psi_{ex} = \frac{Ex_{in} - Ex_L}{Ex_{in}} \quad (16)$$

When the exergy loss or irreversibility of a system is low, the maximum improvement in exergy efficiency is achieved. The rate of exergy improvement potential was calculated using Equation (17) [36–38]:

$$\dot{I}P = (1 - \psi_{ex})(Ex_{in} - Ex_{out}) \quad (17)$$

Finally, the sustainability index (SI) of the drying process was determined by Equation (18) [39]:

$$SI = \frac{1}{1 - \psi_{ex}} \quad (18)$$

2.3.2. Experimental Design and Statistical Analysis

A regression analysis and analysis of variance (ANOVA) were used to develop a complete second-order model for the drying factors of the basil with the hybrid-solar dryer and to evaluate the adequacy of the model and statistical significance. The statistical analysis of the optimization of the drying process of the basil with a hybrid-solar dryer was carried out through the response surface method (RSM). For this purpose, a face-centered central composite design (CCD) was utilized, so the statistical analysis and optimization of the data was carried out by applying the software of Design Expert (version 13.1.0.1, Minneapolis, MN, USA). In the drying process of the basil samples with this kind of dryer,

to investigate the effect of the independent variables on the dependent variables for the experiments, two independent variables of the drying air temperature (40 °C, 55 °C and 70 °C) and three levels of the sample bed thickness (2, 4 and 6 cm), were used on the responses of the drying rate, energy utilization, energy utilization ratio, exergy efficiency, exergy loss rate, exergy improvement potential rate, and sustainability index. The coded levels were (−1), (0), and (1) for the two independent variables of the air temperature and basil bed thickness, each of which was at three different levels, and the dependent variables of the experimental design are listed in Table 1.

Table 1. Experimental layout of independent factors, related levels, criteria and goals utilized for central composite design.

	Parameters	Coded Symbol	Targets	Coded	Actual	Importance
Input parameters	Air temperature, T (°C)	A	In range	−1	2	3
				0	4	
				1	6	
	Bed thickness, BT (cm)	B	In range	−1	40	3
0				55		
1				70		
Responses	Drying rate (g water/g dry matter min)	DR	Maximum		0.1127–0.3227	3
	Energy utilization (kJ/s)	EU	Minimum		0.0124–0.0438	3
	Energy utilization Ratio (-)	EUR	Minimum		0.1181–0.4612	3
	Exergy loss rate (kJ/s)	-	Minimum		0.0078–0.0297	3
	Exergy efficiency (%)	ψ_{ex}	Maximum		31.78–86.55	3
	Improvement potential rate (kJ/s)	IP	Maximum		0.2424–2.549	3
	Sustainability index (-)	SI	Maximum		0.0116–0.0324	3

Central composite design (CCD) experiments (13 cases) were obtained to evaluate the effects of the independent variables on the responses, as shown in Table 2.

Table 2. Experimental central composite design of input and response factors for basil dried under hybrid-solar dryer conditions.

Input Variables				Responses					
Run	Air Temperature °C	Bed Thickness cm	Drying Rate g Water/g Dry Matter min	Energy Utilization kJ/s	Energy Utilization Ratio -	Exergy Loss kJ/s	Exergy Efficiency %	Improvement Potential Rate kJ/s	Sustainability Index -
1	40	2	0.1420	0.0125	0.1181	0.0079	31.79	0.2424	0.0325
2	55	4	0.1958	0.0201	0.2558	0.0175	65.28	1.1358	0.0162
3	55	4	0.1958	0.0201	0.2558	0.0175	65.28	1.1358	0.0162
4	70	4	0.2958	0.0290	0.3357	0.0251	79.53	1.9675	0.0127
5	55	4	0.1958	0.0201	0.2558	0.0175	65.28	1.1358	0.0162
6	70	6	0.2219	0.0418	0.4612	0.0298	86.56	2.5495	0.0117
7	55	6	0.1561	0.0276	0.3394	0.0213	71.23	1.5069	0.0148
8	40	6	0.1127	0.0196	0.1777	0.0122	42.24	0.5050	0.0242
9	55	2	0.2132	0.0152	0.1915	0.0106	55.12	0.7501	0.0182
10	55	4	0.1958	0.0201	0.2558	0.0175	65.28	1.1358	0.0162
11	40	4	0.1315	0.0155	0.1399	0.0092	37.58	0.3358	0.0273
12	55	4	0.1958	0.0201	0.2558	0.0175	65.28	1.1358	0.0162
13	70	2	0.3227	0.0225	0.2511	0.0195	70.40	1.3555	0.0144

A coefficient of determination (R^2), adjusted regression coefficient (Adj- R^2), predicted regression coefficient (Predicted- R^2), and analysis of variance (ANOVA) with statistical and response plots were used to analyze the results and evaluate the significance and accuracy of the model. The specific RSM was used and evaluated in relation to the actual data along with the corresponding F and p values at the 95% confidence level.

After the drying experiments, the data (independent and interactive effects of the variables on responses) were fitted using a second-order polynomial equation [40,41]:

$$Y = \alpha_0 + \sum_{i=1}^k \alpha_i x_i + \sum_{i=1}^k \alpha_{ii} x_i^2 + \sum_{i=1}^{k-1} \sum_{j=1}^k \alpha_{ij} x_i x_j \quad (19)$$

The total desirability function (D) was the evaluation factor to find the optimal points, which was calculated using the geometric mean of eight individual desirability functions as follows [14]:

$$D = (d_1 \times d_2 \times d_3 \times d_4 \times d_5 \times d_6 \times d_7)^{\frac{1}{7}} \quad (20)$$

Overall, the range and purpose of the responses were determined to maximize the amount of exergy efficiency (d_1), exergy improvement potential rate (d_2) sustainability index (d_3), and drying rate (d_4), and to minimize the exergy loss rate (d_5), energy utilization (d_6), and energy utilization ratio (d_7) to perform the optimization process.

3. Results and Discussion

3.1. The Influence of Air Temperature and Bed Thickness on the Drying Rate

Figure 2 illustrates the drying rate (DR) of the basil samples at different drying air temperatures and bed thicknesses during the drying process. As can be seen in Figure 2, there were two distinct periods in the drying rate curves.

The first period included a sharp acceleration corresponding to the initial temperature. This increase occurred at the beginning of the drying process. It was similar to the process observed by Prashob et al. [42] at the beginning of drying shrimp at different temperatures. This was attributed to the increased driving force for the migration of moisture inside the material due to higher drying temperatures. During the descending period, a lower rate was observed along with the plot. The moisture movement at a decreasing rate time was determined by molecular diffusion, which was the predominant physical mechanism in this period. As the drying time increased, the moisture content of the samples decreased exponentially until the equilibrium moisture content was reached. In the first few hours of drying, the moisture drop was faster, but later the moisture drop was slower because the moisture moved from the interior of the material to the outer surface and then evaporated [43]. The lowest drying time for the basil samples was obtained at a temperature of 70 °C and a bed thickness of 2 cm, whereas the highest value was achieved at the temperature of 40 °C and a bed thickness of 6 cm; thus, the drying rate increased as the sample thickness increased. Zheng et al. [44] reported that the moisture content in all the biological products decreased during the drying process. In other words, the water moved from points with higher moisture to points with lower moisture during the drying time, and the movement of water from the sample to the surface of the product was controlled by molecular diffusion. These results are consistent with the findings of the previous researchers, namely, Karami et al. [33] for rosemary in a solar-convection dryer, Moussaoui et al. [45] for apple in a hybrid solar-electrical forced convection dryer and Tagnamas et al. [46] for carob seeds in a convective solar dryer.

3.2. Drying Rate

Table 3 shows the predicted effects of the independent parameters and their interactions for the ANOVA. The results demonstrate that the linear effects with the value of (p -value < 0.0001) interactions (p -value = 0.0001), and the quadratic (p -value = 0.0006) for the air temperature (A^2) and (p -value < 0.0030) for the bed thickness (B^2), were significant, and this was in a good agreement with the results of Karami et al., [7]. In Table 3, the results of the lack of fit were not significant ($p \geq 0.05$). The drying results showed no significant lack of fit, indicating that the model was well fitted. Based on the coefficient of variation (CV) of 2.35%, it can be seen that the selected model has a good signal-to-noise ratio and can be used to move around the design space [23].

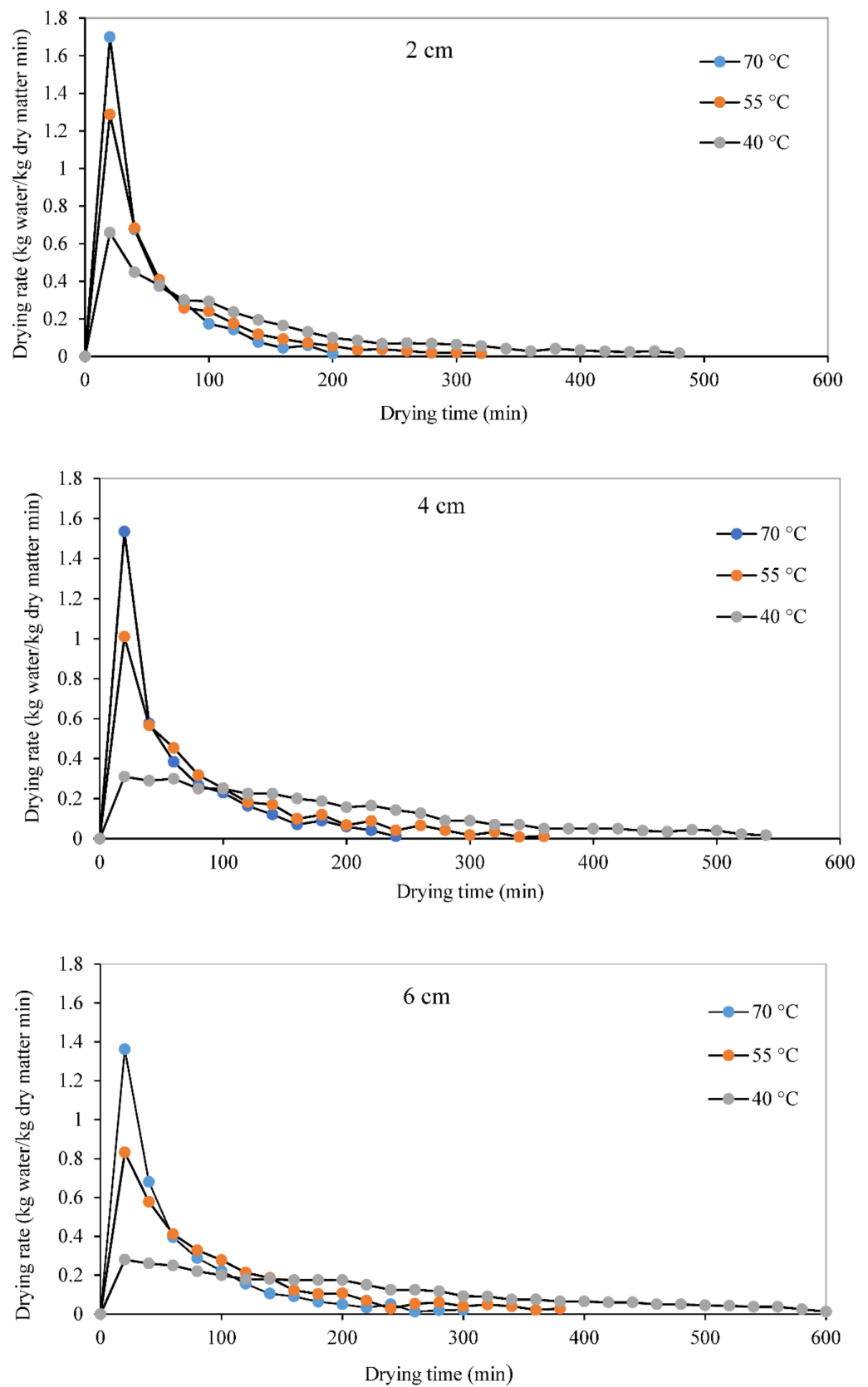


Figure 2. Changes in the drying rate of basil during the drying period at different temperatures and bed thicknesses.

Table 3. ANOVA analysis for the response of drying rate of quadratic model of RSM.

Source	Sum of Squares	df	Mean Square	F-Value	p-Value	
Model	0.0424	5	0.0085	390.54	<0.0001 **	significant
A-Air temperature	0.0344	1	0.0344	1584.10	<0.0001 **	
B-Bed thickness	0.0058	1	0.0058	268.99	<0.0001 **	
AB	0.0013	1	0.0013	59.04	0.0001 **	
A ²	0.0008	1	0.0008	35.00	0.0006 **	
B ²	0.0004	1	0.0004	19.70	0.0030 **	
Residual	0.0002	7	0.0000			
Lack of Fit	0.0002	3	0.0001			
Pure Error	0.0000	4	0.0000			
Cor Total	0.0425	12				
C.V.%	2.35					

Note: ** denotes 1% level of significance.

In general, the fit of the models was tested using an ANOVA, and the results showed that the equation adequately represented the true relationship between the two independent variables and responses (Tables 3 and 4).

Table 4. Summarized statistical data of predictive models for drying rate under hybrid-solar dryer.

Source	Std. Dev.	R ²	Adjusted R ²	Predicted R ²	PRESS	
Linear	0.0152	0.9456	0.9347	0.8697	0.0055	
2FI	0.0107	0.9757	0.9676	0.9479	0.0022	
Quadratic	0.0047	0.9964	0.9939	0.9640	0.0015	Suggested
Cubic	0.0010	0.9999	0.9997	0.9866	0.0006	Aliased

The results in Table 4 show that the quadratic model with an R² value (0.9964), predicted R² (0.9640), adjusted R² (0.9939), and PRESS (0.0015) was the best model for the drying rate. Additionally, the cubic model was considered to be over fitted compared to the other evaluated models.

Equation (21) shows the fit of the quadratic polynomial model with the independent parameters to the drying rate:

$$Dr = 0.1962 + 0.0757A - 0.0312B - 0.0179AB + 0.0166A^2 - 0.0124B^2 \quad (21)$$

However, the positive sign of the estimated regression coefficients from the central composite design model indicated the direct effect of the independent parameters on the response variable (Dr), while the negative sign indicated the reverse effect of these parameters on the drying rate. The coefficients also indicated that the independent variable of the drying air temperature with the highest value (0.0757), had the greatest effect on the dependent variable (drying rate) [47].

The combined effect of the two factors including the bed thickness and drying air temperature on the drying rate is shown in Figure 3a as a 3D response surface and contour plot for the quadratic polynomial model.

The drying rate not only increased with an increasing drying air temperature (A) but also decreased more with a decreasing basil bed thickness when it was less than 4 cm (Figure 3a,b).

As can be seen in Figure 3b for the contour plot of the independent and dependent parameters, higher drying air temperatures resulted in the lowest drying time rates. Both the air temperature and bed thickness were found to affect the drying rate simultaneously, but the drying air temperature had a greater effect on the drying rate than the bed thickness. Moreover, the results showed that the drying rate was directly related to the drying air temperature and inversely related to the bed thickness; therefore, the drying rate increased with an increasing drying air temperature and decreasing bed thickness. Similar results were obtained by Golpour et al. [48] and Demirpolat et al. [49].

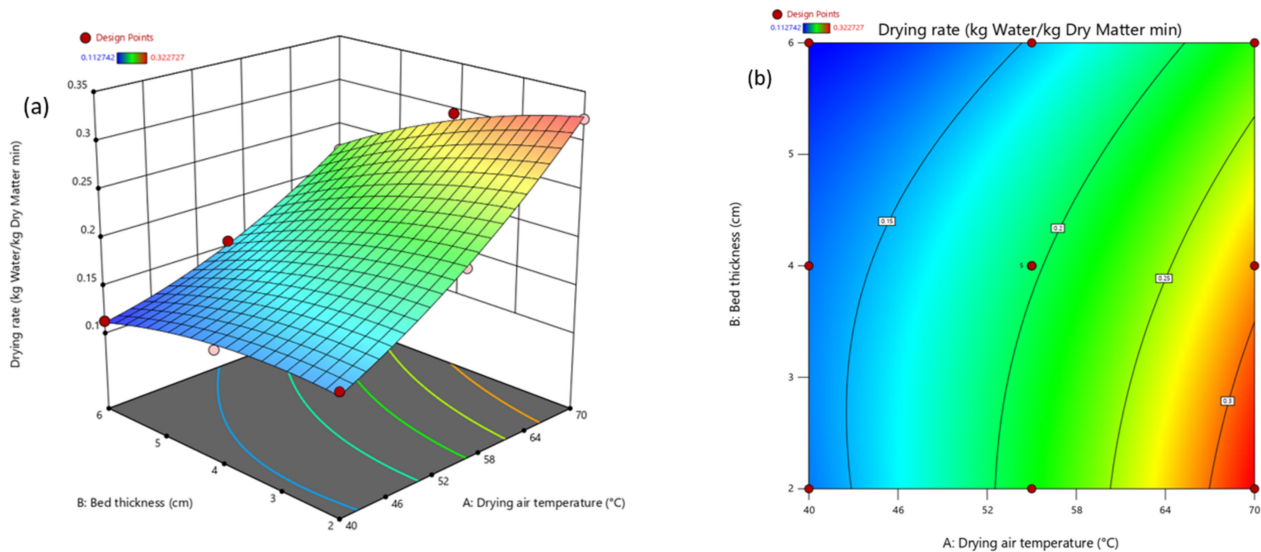


Figure 3. The effect of bed thickness and air temperature on the predicted response surface of drying rate (kg water/kg dry matter min), (a) 3D response surface and (b) 2D contour plot.

3.3. Energy Utilization

In Table 5, the results of the statistical analysis parameters resulting from the analysis of variance for the input parameters of bed thickness and drying air temperature on the energy utilization (EU) are reported.

Table 5. ANOVA analysis for the response of energy utilization of quadratic model of RSM.

Source	Sum of Squares	df	Mean Square	F-Value	<i>p</i> -Value	
Model	0.0007	5	0.0001	344.42	<0.0001 **	significant
A-Air temperature	0.0003	1	0.0003	892.68	<0.0001 **	
B-Bed thickness	0.0003	1	0.0003	640.80	<0.0001 **	
AB	0.0000	1	0.0000	95.33	<0.0001 **	
A ²	0.0000	1	0.0000	42.82	0.0003 **	
B ²	6.494×10^{-6}	1	6.494×10^{-6}	16.61	0.0047 **	
Residual	2.736×10^{-6}	7	3.909×10^{-7}			
Lack of Fit	2.736×10^{-6}	3	9.120×10^{-7}			
Pure Error	0.0000	4	0.0000			
Cor Total	0.0007	12				
C.V.%	2.86					

Note: ** denotes 1% level of significance.

The results showed that the selected model perfectly predicted the response of the energy utilization ($p < 0.05$). The values of F for the selected model were 342.42 and the p -value < 0.0001 ; therefore, the lack of fit was insignificant showing a significant model (Table 5). There is only a 0.01% possibility that a high value of F is due to creating noise. In other words, the related model had a good performance for estimating the relevant response based on the factors studied and was statistically significant; however, it is worth noting that the p -values for the independent variables of the drying air temperature (A), bed thickness (B), and their interaction (AB) were $p < 0.0001$, so that the values for the quadratic values of these parameters (A² and B²) were 0.0003 and 0.0047, respectively. This shows that these parameters had a significant effect on the response of the energy utilization at a confidence level of 95% ($p < 0.05$) (Table 5).

An analysis of variance according to Table 5 showed energy utilization with the lowest value of the variation coefficient (C.V. = 2.86%), indicating that the standard deviation (percentage of the mean) increased the reliability of the experiment [20,50].

According to the model developed for energy utilization, the quadratic model with R² (0.9960), adjusted R² (0.9931), predicted R² (0.9598), and a value of PRESS = 0.0000 was

significant at $p < 0.01$. The selected model had a good fit with no significant lack of fit. The difference between the predicted and adjusted R^2 values was less than 0.20, which was in a reasonable fit (Table 6).

Table 6. Summarized statistical data of predictive models for energy utilization under hybrid-solar dryer.

Source	Std. Dev.	R^2	Adjusted R^2	Predicted R^2	PRESS	
Linear	0.0028	0.8869	0.8642	0.7184	0.0002	
2FI	0.0021	0.9420	0.9227	0.6973	0.0002	
Quadratic	0.0006	0.9960	0.9931	0.9598	0.0000	Suggested
Cubic	0.0002	0.9997	0.9993	0.9663	0.0000	Aliased

The results of this study on the optimization of the energy utilization parameter for basil drying showed that the extracted mathematical model (Equation (22)) was based on effective coding factors, interactions, and quadratic effects. By default, the high values were coded as +1 and low values as -1 . Generally, a coded Equation (22) can be used to determine the relative effect of factors by comparing their coefficients [51]:

$$EU = 0.0200 + 0.0076A + 0.0065B + 0.0031AB + 0.0025A^2 + 0.0015B^2 \quad (22)$$

From the high quadratic polynomial model, it can be seen that all the parameters had a positive effect on energy utilization, so that the air temperature had the highest effect with a coefficient of 0.0076 compared to all the factors and terms in the regression model.

This 3D diagram and 2D contour of the response surface of the energy utilization interaction with the drying air temperature and bed thickness for drying basil are shown in Figure 4a,b.

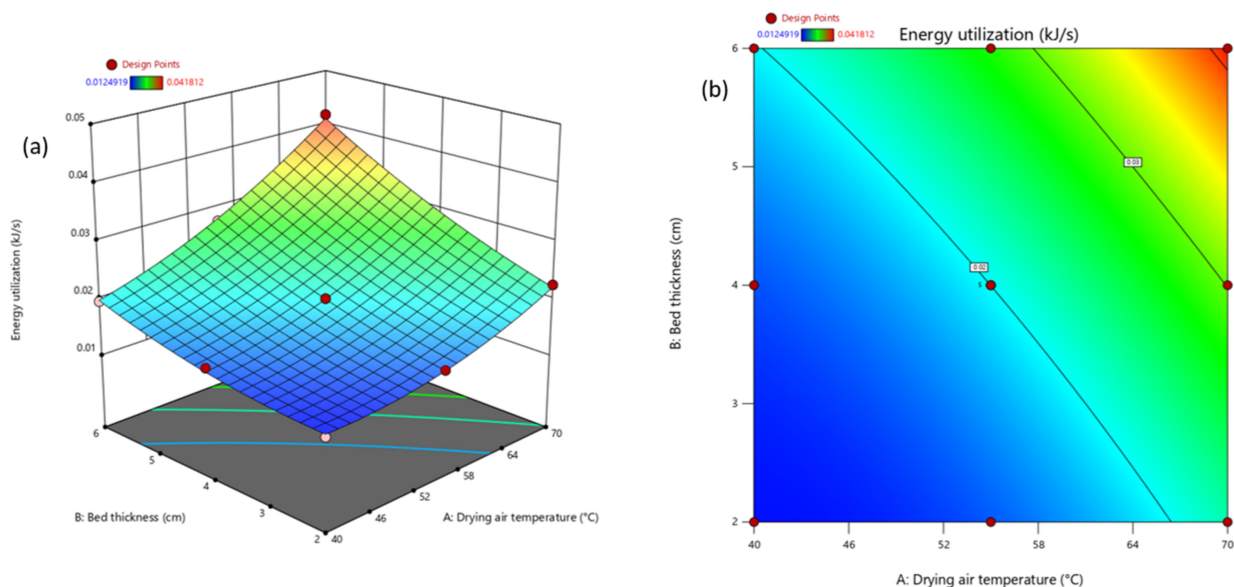


Figure 4. The effect of bed thickness and air temperature on the predicted response surface of energy utilization, (a) 3D response surface and (b) 2D contour plot.

According to the figures, the maximum value of EU at 70 °C and a bed thickness of 6 cm, and the minimum EU value at 40 °C and a bed thickness of 2 cm were 0.041 and 0.012 kJ/s, respectively. The effects of the drying air temperature and the bed thickness variables on the EU value can be found in this figure. Figure 4a,b shows that both the drying air temperature and the bed thickness affected the EU simultaneously. In other

words, the EU increased with an increasing air temperature and bed thickness; thus, the temperature of the air and the bed thickness were directly related to the EU. In this regard, the increase in energy utilization may be because the enthalpy supplied increased with the increasing drying air temperature and bed thickness, which in turn led to an increase in the energy utilization, since the EU is directly related to enthalpy [33]. Moreover, these results agreed well with Das et al. [52] and Pattanayak et al. [53].

3.4. Energy Utilization Ratio

With respect to Table 7 for the variance analysis, the F value of the output variable (utilized energy rate) was 1118.73, while the lack of fit of this model with the satisfaction coefficient of determination (R^2) was not significant at all.

Table 7. ANOVA analysis for the response of energy utilization ratio of quadratic model of RSM.

Source	Sum of Squares	df	Mean Square	F-Value	p-Value	
Model	0.0980	5	0.0196	1118.73	<0.0001 **	significant
A-Air temperature	0.0625	1	0.0625	3565.86	<0.0001 **	
B-Bed thickness	0.0291	1	0.0291	1658.77	<0.0001 **	
AB	0.0057	1	0.0057	323.33	<0.0001 **	
A ²	0.0007	1	0.0007	39.38	0.0004 **	
B ²	0.0004	1	0.0004	22.18	0.0022 **	
Residual	0.0001	7	0.0000			
Lack of Fit	0.0001	3	0.0000			
Pure Error	0.0000	4	0.0000			
Cor Total	0.0981	12				
C.V.%	1.65					

Note: ** denotes 1% level of significance.

As a result, the model was appropriate with a p -value < 0.0001. At the 95% confidence level, the p -value of the model was less than 0.05, which means that the model terms were significant (Table 7). The results showed that air temperature (A), bed thickness (B), and their interactions (AB) ($p < 0.0001$) had a significant effect on the EUR. In addition, the quadrature effects of the drying air temperature (A^2) and bed thickness (B^2) were significant at the 95% probability level with p -values of 0.0004 and 0.0022, respectively (Table 7). Nevertheless, the experimental data were well expressed by the model, and estimated the energy utilization ratio very closely while the p -value of the model with a low C.V. value (1.65%) was less than 10% [54].

The results of the model responses are summarized in Table 8.

Table 8. Summarized statistical data of predictive models for energy utilization ratio under hybrid-solar dryer.

Source	Std. Dev.	R ²	Adjusted R ²	Predicted R ²	PRESS	
Linear	0.0257	0.9329	0.9194	0.8173	0.0179	
2FI	0.0101	0.9906	0.9875	0.9807	0.0019	
Quadratic	0.0042	0.9988	0.9979	0.9878	0.0012	Suggested
Cubic	0.0017	0.9998	0.9996	0.9825	0.0017	Aliased

According to the results, the high values of adjusted R^2 and R^2 show that the developed models were suitable for predicting the energy utilization ratio so that the predicted values of R^2 were close to the adjusted R^2 ; however, the analysis of variance showed that the quadratic model was the best model to explain the energy utilization ratio, as shown in Table 8. It is important to note that the values of R^2 and adjusted R^2 , predicted R^2 , and PRESS for the selected model to estimate the response of the energy utilization ratio were 0.9988, 0.9979, 0.9878, and 0.0012, respectively, as shown in Table 8.

Using the response surface method model and the air temperature and bed thickness parameters, the energy utilization ratio was predicted. Based on this method, all parameters, their interactions, and their quadratic terms are given in the following equation:

$$EUR = 0.2552 + 0.1020A + 0.0696B + 0.0376AB - 0.158A^2 + 0.0119B^2 \quad (23)$$

The drying air temperature (A), sample bed thickness (B), their interaction effects (AB), and quadratic value of bed thickness (B^2) had a direct relation with the EUR and the drying air temperature had the highest effect between the parameters and the terms. In contrast, the quadratic term of the drying air temperature (A^2) was inversely related to this response.

Figure 5 showed the three-dimensional curve of the response surface and the contour of the energy utilization ratio of the basil drying process.

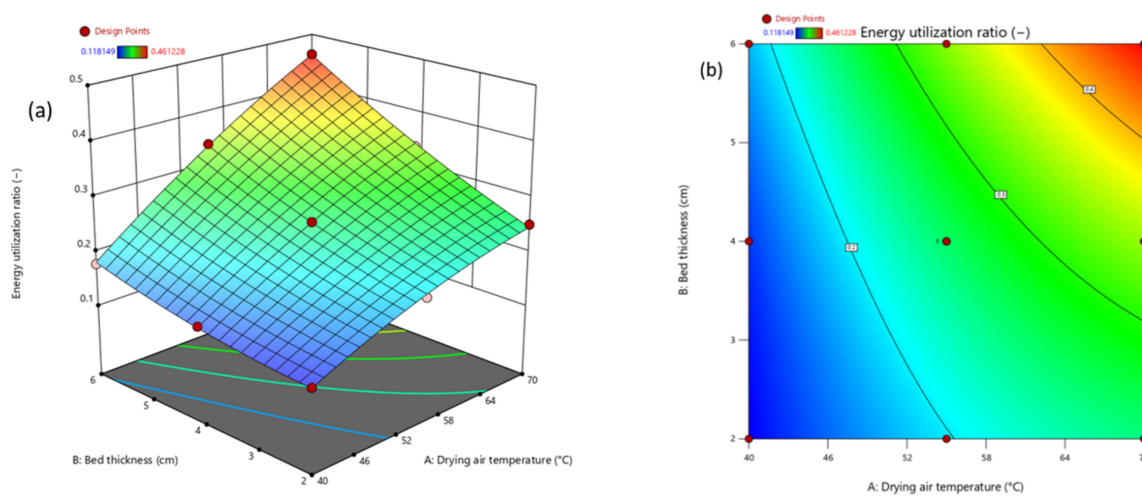


Figure 5. The effect of bed thickness and air temperature on the predicted response surface of energy utilization ratio, (a) 3D response surface and (b) 2D contour plot.

Generally, Figure 5 reports the values of the energy utilization ratio for the test variables of the drying air temperature and bed thickness at each point of the indicated area and their interactions. As shown in Figure 5b, the maximum EUR value at 70 °C and a bed thickness of 6 cm, and the minimum EUR value at 40 °C and a bed thickness of 2 cm were 0.461 and 0.1181, respectively. According to the reported figures, the air temperature and bed thickness had a significant effect on the EUR values, so that the EUR increased directly with the drying air temperature and bed thickness. The RSM model also supports this claim, but the influence of air temperature was more than the bed thickness on the EUR value, as its coefficient was the highest in the relevant model. These results were similar to Das et al. [52], and a good agreement was found. Erick César et al. [8] studied the energy and exergy of a mixed-mode solar dryer for pear slices. They reported a highest average energy utilization ratio of 29.1% in an indirect-mode natural convection.

3.5. Exergy Efficiency

Exergy efficiency can be evaluated using the results of the analysis of variance from Table 9. As a result, the selected model with a p -value < 0.0001, and the effects of temperature (A) and bed thickness (B) were significant at the 1% and 5% levels, respectively, and the second-degree term of the drying air temperature (A^2) with a p -value < 0.0001 and the interaction effect of the drying air temperature and bed thickness (AB) with a p -value < 0.0064, were significant only at the 5% level, while the second-degree term of the bed thickness (B^2) had a p -value < 0.0129. The p -values were obtained for these parameters: 4722.40, 552.42, 186.49, 14.76, and 10.98, respectively (Table 9). The non-significance of the

lack of fit parameter and the low value of the variation coefficient (C.V. = 1.20%) indicated that the chosen model was suitable for the estimation of the exergy efficiency.

Table 9. ANOVA analysis for the response of exergy efficiency of quadratic model of RSM.

Source	Sum of Squares	df	Mean Square	F-Value	p-Value	
Model	3060.98	5	612.20	1112.18	<0.0001 **	significant
A-Air temperature	2599.44	1	2599.44	4722.40	<0.0001 **	
B-Bed thickness	304.08	1	304.08	552.42	<0.0001 **	
AB	8.13	1	8.13	14.76	0.0064 **	
A ²	102.65	1	102.65	186.49	<0.0001 **	
B ²	6.04	1	6.04	10.98	0.0129 *	
Residual	3.85	7	0.5504			
Lack of Fit	3.85	3	1.28			
Pure Error	0.0000	4	0.0000			
Cor Total	3064.84	12				
C.V.%	1.20					

Note: *, ** denote 5 and 1% levels of significance, respectively.

In evaluating the significance of all terms of the quadratic model for estimating the exergy efficiency, it was found that the model with a value of $R^2 = 0.9987$ had a good performance for fitting the experimental and predicted data, which represented only 0.23% of the total changes not accounted for by the RSM model (Table 10).

Table 10. Summarized statistical data of predictive models for exergy efficiency under hybrid-solar dryer.

Source	Std. Dev.	R ²	Adjusted R ²	Predicted R ²	PRESS	
Linear	4.02	0.9474	0.9368	0.8954	320.44	
2FI	4.13	0.9500	0.9334	0.7890	646.62	
Quadratic	0.7419	0.9987	0.9978	0.9885	35.36	Suggested
Cubic	0.4797	0.9996	0.9991	0.9564	133.70	Aliased

For this selected model, adjusted R^2 , predicted R^2 , and PRESS values were 0.9978, 0.9885, and 35.36, respectively, which were statistically acceptable values for predicting the exergy efficiency (Table 10).

In Equation (24), the results of the obtained quadratic polynomial model were shown in relation to the response of the exergy efficiency and the independent variables temperature (A) and sample bed thickness (B):

$$EX_{eff} = 65.10 + 20.81A + 7.12B + 1.43AB - 6.10A^2 - 1.48B^2 \quad (24)$$

Equation (24) shows that all parameters of the independent variables (A) and (B), their interaction effects (AB), and their second-order parameters (A²) and (B²) were significant. Accordingly, the temperature and the thickness of the sample bed and their interactions had a positive effect on the exergy efficiency, while the second-order term had the opposite effect. In general, the drying air temperature had a greater effect on exergy efficiency than the sample bed thickness.

Figure 6 shows the interactions between the parameters of drying air temperature and thickness of the basil sample during the drying process in the form of a 3D reaction surface curve of the quadratic polynomial model and a 2D contour of the exergy efficiency.

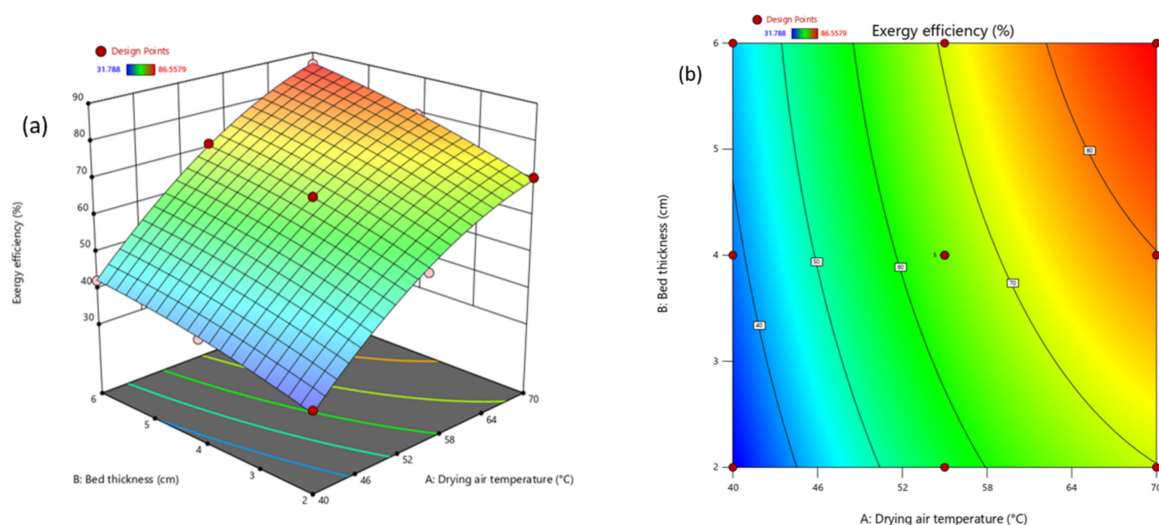


Figure 6. The effect of bed thickness and air temperature on the predicted response surface of exergy efficiency, (a) 3D response surface and (b) 2D contour plot.

The average exergy efficiency values ranged from 31.78% at 40 °C and 2 cm sample bed thickness to 86.56% at 70 °C and 6 cm layer thickness of the sample bed (Figure 6a,b). In this study, higher exergy efficiency values (31.78–86.56%) were obtained than in the study of Yogendrasidhar and Setty [12] on fenugreek seed drying. This difference could have been caused by the application of solar energy to the drying kinetics of the basil. Hybrid-solar drying increased the surface temperature of the basil sample, the moisture diffusion in and on the surface of the samples and a higher moisture pressure, that caused a shorter drying time compared to hot air drying. As a result, more evaporation took place, leading to more exergy and a better energy efficiency. In other words, as the bed thickness increased, so did the inlet exergy flow of the hybrid-solar dryer. As shown in Figure 6a,b, similar results were obtained for the air inlet temperature parameter. From the figures, it can be seen that both the drying air temperature and the bed thickness affected the exergetic efficiency. In other words, the higher the drying air temperature and bed thickness, the higher the exergy efficiency. Consequently, the air temperature and bed thickness were directly related to the exergy efficiency (Figure 5a,b). Similar results were obtained by Yogendrasidhar and Setty [12] for drying kudu millet and Suherman et al. [55] for drying cassava starch with a hybrid dryer, where the exergy efficiency increased with an increasing air temperature. Erick César et al. [8] studied the energy and exergy of a mixed-mode solar dryer for pear slices and they reported that the exergy efficiency values of the dryer chamber were 65.2% in a mixed-mode natural convection, while the lowest were in a mixed-mode forced convection (54.4%).

3.6. Exergy Loss Rate

Table 11 illustrates that the analysis of variance extracted from the response surface optimization method for the exergy loss rate, showing the model chosen for this process for drying basil was highly significant with a p -value < 0.0001 and an F-value of 172.03, with only a 0.01% probability that the F-value with this high value was due to noise ($p < 0.01$).

Table 11. ANOVA analysis for the response of exergy loss of 2F model of RSM.

Source	Sum of Squares	df	Mean Square	F-Value	p-Value	
Model	0.0005	3	0.0002	172.03	<0.0001 **	significant
A-Air temperature	0.0003	1	0.0003	384.40	<0.0001 **	
B-Bed thickness	0.0001	1	0.0001	121.82	<0.0001 **	
AB	8.692×10^{-6}	1	8.692×10^{-6}	9.86	0.0119 *	
Residual	7.931×10^{-6}	9	8.812×10^{-7}			
Lack of Fit	7.931×10^{-6}	5	1.586×10^{-6}			
Pure Error	0.0000	4	0.0000			
Cor Total	0.0005	12				
C.V.%	5.47					

Note: *, ** denote 5 and 1% levels of significance, respectively.

In this case, only the independent variables of the drying air temperature (A), bed thickness (B), and their interactions (AB) on the exergy losses were highly significant at the 95% confidence level ($p < 0.05$); however, the non-significance of the lack of fit indicated a disagreement with the magnitude of the pure error, indicating that the model for basil drying obtained by the response surface method fit the experimental data well. A non-significant measure of the lack of fit showed it was a suitable model to predict the related response, which was in agreement with Kumar, Prasad and Murthy [56], Nwakuba [57], and Uzoma, Nwakuba and Anyaoha [58]. After the analysis of variance, the coefficient of variation (C.V.%) for these experimental data was 5.47% (Table 11).

According to the results of the analysis of variance in Table 12, the 2FI model with the R^2 of 0.9829, adjusted R^2 of 0.9771, predicted R^2 of 0.9458 and PRESS of 0.0000 showed a suitable fit and a very good correlation with the values of the predicted exergy losses, indicating this parameter could have caused a higher proportion of changes in the experiment.

Table 12. Summarized statistical data of predictive models for exergy loss under hybrid-solar dryer.

Source	Std. Dev.	R^2	Adjusted R^2	Predicted R^2	PRESS	
Linear	0.0013	0.9641	0.9569	0.9126	0.0000	
2FI	0.0009	0.9829	0.9771	0.9458	0.0000	Suggested
Quadratic	0.0010	0.9859	0.9758	0.8714	0.0001	
Cubic	0.0006	0.9955	0.9891	0.4716	0.0002	Aliased

With a value difference of less than 0.20 between the adjusted R^2 of 0.9771 and the predicted R^2 of 0.9458, the fit of the model shows that it was properly used to predict the exergy loss (Table 12).

Equation (25) presents a quadratic polynomial model for exergy loss during the hybrid-solar drying of the basil samples with different drying variables:

$$Ex_{loss} = 0.0171 + 0.0075A + 0.0042B + 0.0015AB \quad (25)$$

According to the above equation, the drying air temperature with the highest positive coefficient of 0.0075 was the most effective parameter in reducing the exergy losses, while among the terms, the sample thickness parameter with a positive coefficient of 0.0042 reduced the exergy loss rate with the lowest effect on the loss.

Figure 7 shows the interaction effect of the hybrid-solar dryer input variables (drying air temperature and bed thickness) on the exergy loss rate as a 3D response surface and 2D contour plot.

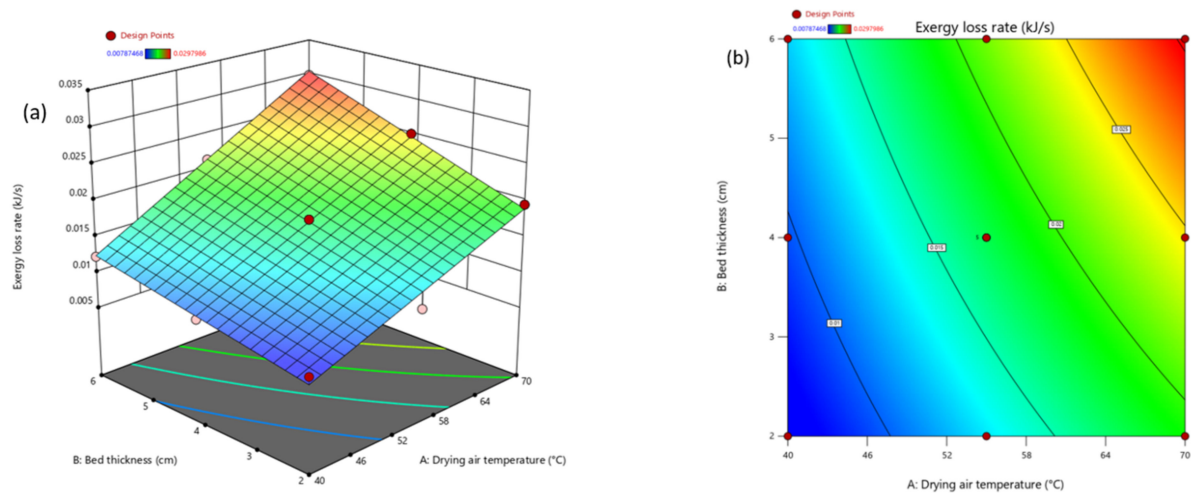


Figure 7. The effect of bed thickness and air temperature on the predicted response surface of exergy loss rate, (a) 3D response surface and (b) 2D contour plot.

As the air velocity (1 m/s), drying air temperature (A), and bed thickness (B) of the basil drying process increased, the amount of exergy loss increased, indicating that the drying air temperature and bed thickness had a direct influence on the exergy loss in this study (Figure 7a). The results showed that the lowest amount of exergy loss was 0.0078 kJ/s, obtained at 40 °C and a bed thickness of 2 cm, while the highest values of the same parameter (0.0298) were obtained at 70 °C and a bed thickness of 6 cm, respectively (Figure 7a,b).

3.7. Exergetic Improvement Potential Rate

Table 13 shows the results of the ANOVA for the exergy improvement potential response rate by the second-order polynomial model (Equation (26)) for all the independent variables and their interactions.

Table 13. ANOVA analysis for the response of improvement potential rate of quadratic model of RSM.

Source	Sum of Squares	df	Mean Square	F-Value	p -Value	
Model	4.86	5	0.9717	4705.99	<0.0001 **	significant
A-Air temperature	3.82	1	3.82	18,514.77	<0.0001 **	
B-Bed thickness	0.8165	1	0.8165	3954.49	<0.0001 **	
AB	0.2169	1	0.2169	1050.39	<0.0001 **	
A^2	0.0017	1	0.0017	8.33	0.0234 *	
B^2	8.629×10^{-6}	1	8.629×10^{-6}	0.0418	0.8438 ns	
Residual	0.0014	7	0.0002			
Lack of Fit	0.0014	3	0.0005			
Pure Error	0.0000	4	0.0000			
Cor Total	4.86	12				
C.V.%	1.25					

Note: *, ** and ns denote 5 and 1% levels of significance and not significant, respectively.

The analysis of variance evaluated by the Design-Expert software using the response level method for the exergy improvement potential rate resulted in an F-value of 4705.99, which determined the variance of the total improvement potential data to the mean (Table 13). Additionally, the model's low p -value < 0.0001 indicated that the selected model was highly significant in predicting this parameter relative to the levels of the independent variables ($p < 0.01$). In this case, A , B , AB , A^2 , were the significant variables of the model at 95% ($p < 0.05$) and 99% ($p < 0.01$), confidence levels, respectively, so that the A^2 with the value ($p = 0.0234$) was significant only at a 95% confidence level ($p < 0.05$) (Table 13). According to the results, B^2 with a value ($p = 0.8438$) was also the only non-significant variable in the model ($p > 0.05$). The ANOVA also showed that the lack of fit for the models at the response

level of the exergy improvement potential rate was not significant at the 95% confidence level with a coefficient of variation of 1.25%, which also indicated the proper performance of the corresponding model (Table 13).

The results of the ANOVA for the quadratic model of exergetic improvement potential rate, R^2 of 0.9997, and an adjusted and predicted R^2 of 0.9995 and 0.9971, respectively, are presented in Table 14.

Table 14. Summarized statistical data of predictive models for improvement potential rate under hybrid-solar dryer.

Source	Std. Dev.	R^2	Adjusted R^2	Predicted R^2	PRESS	
Linear	0.1485	0.9546	0.9456	0.8701	0.6314	
2FI	0.0199	0.9993	0.9990	0.9964	0.0173	
Quadratic	0.0144	0.9997	0.9995	0.9971	0.0139	Suggested
Cubic	0.0069	1.0000	0.9999	0.9942	0.0280	Aliased

According to the results, there was a very significant model, so that many experiments were accurate and reliable; therefore, the resulting quadratic model had a good relationship between the set of independent variables and the corresponding response. In this analysis, the values of the standard deviation and PRESS were found to be 0.0144 and 0.0139, respectively (Table 14).

By evaluating the multiple regression on the experimental data (the variables of the drying process for basil), a quadratic polynomial equation derived from the response surface methodology of Equation (26), was found to express the exergetic improvement potential rate:

$$IP = 1.13 + 0.7982A + 0.3689B + 0.2329AB + 0.0250A^2 \quad (26)$$

According to the above equation and the corresponding coefficients of each parameter, the term of the linear parameter of the drying air temperature (A), the thickness of the sample bed (B) for the drying process, the terms of interaction (AB), and their quadratic (A^2) and (B^2) were directly related to the exergetic improvement potential rate. Since the coefficients of all the terms were positive, the drying air temperature was more effective than the variable of the sample bed thickness due to a higher coefficient of 0.7982.

A 3D plot and 2D contour curve of the combined effects of the independent variables (the drying air temperature and sample bed thickness) on the dependent variable (exergetic improvement potential rate) were generated. These combined and interactive effects of the independent variables are shown in Figure 8a,b.

The values obtained from the analysis of the exergetic improvement potential rate using Equation (17) ranged from 0.242 kJ/s (at 40 °C and a 2 cm bed thickness) to 2.549 kJ/s (at 70 °C and a bed thickness of 6 cm), which were less than the same parameter value reported by Afzali et al. [14] for white mulberry drying; however, the exergetic improvement potential rate increased directly with an increasing drying air temperature and sample thickness. Similarly, Beigi [59] reported a potential IP of between 12.28–36.39 J/s. Karami et al. [33] also found that the average IP values varied from 0.321 to 2.141 kJ/s. Beigi et al. [38] reported that the range of IP values was between 17.27 to 66.04 J/s.

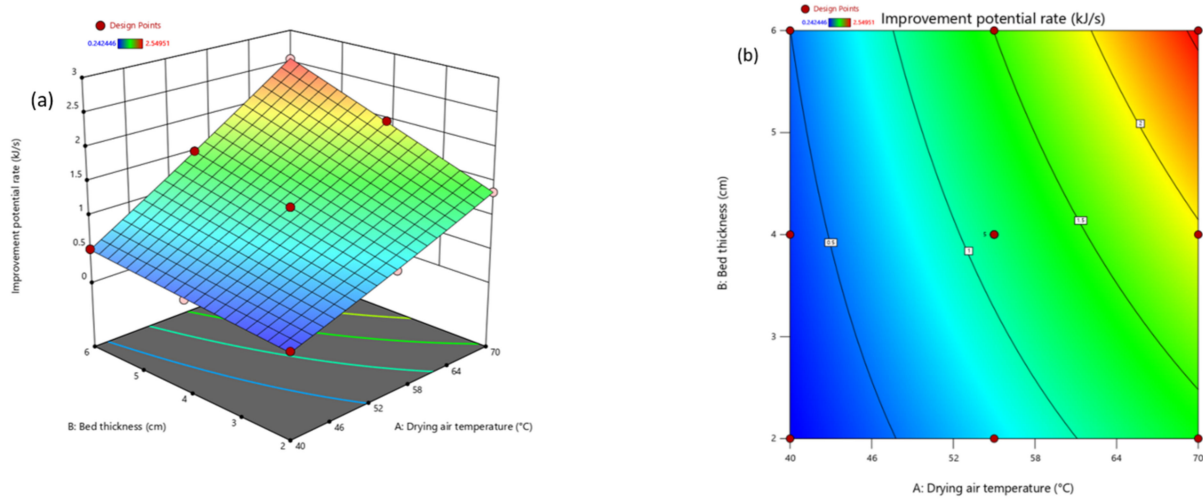


Figure 8. The effect of bed thickness and air temperature on the predicted response surface of improvement potential rate, (a) 3D response surface and (b) 2D contour plot.

3.8. Sustainability Index

Tables 15 and 16 show the results of the regression and variance analyses for the experiments and the evaluation of the corresponding models.

Table 15. ANOVA analysis for the response of sustainability index of quadratic model of RSM.

Source	Sum of Squares	df	Mean Square	F-Value	p-Value	
Model	0.0004	5	0.0001	358.42	<0.0001 **	significant
A-Air temperature	0.0003	1	0.0003	1385.15	<0.0001 **	
B-Bed thickness	0.0000	1	0.0000	139.29	<0.0001 **	
AB	7.594×10^{-6}	1	7.594×10^{-6}	30.84	0.0009 **	
A ²	0.0000	1	0.0000	183.75	<0.0001 **	
B ²	6.075×10^{-7}	1	6.075×10^{-7}	2.47	0.1602 ns	
Residual	1.723×10^{-6}	7	2.462×10^{-7}			
Lack of Fit	1.723×10^{-6}	3	5.745×10^{-7}			
Pure Error	0.0000	4	0.0000			
Cor Total	0.0004	12				
C.V.%	2.73					

Note: ** and ns denote 1% levels of significance and not significant, respectively.

Table 16. Summarized statistical data of predictive models for sustainability index under hybrid-solar dryer.

Source	Std. Dev.	R ²	Adjusted R ²	Predicted R ²	PRESS	
Linear	0.0026	0.8473	0.8168	0.6756	0.0001	
2FI	0.0026	0.8645	0.8193	0.3913	0.0003	
Quadratic	0.0005	0.9961	0.9933	0.9612	0.0000	Suggested
Cubic	0.0001	0.9998	0.9994	0.9722	0.0000	Aliased

Table 15 shows that the proposed model for predicting the response of the sustainability index was highly significant ($p < 0.0001$). The same results showed that the F value for the present model was 358.42. On the other hand, the analysis of variance (ANOVA) and regression revealed that all terms (A, B, AB, A²) based on the probability ($p < 0.01$), except for the quadratic term of sample thickness (B²) with ($p > 0.05$), were highly significant. Reducing the size of a model may be beneficial if it contains many meaningless terms. Based on the results obtained to evaluate the sustainability index, both the drying air temperature and sample bed thickness had a positive effect on this response. In other words, the sustainability index increased when these factors increased. The coefficient of variation in this analysis was 2.73%.

In addition, the statistical parameters for the quadratic *SI* response-level model were 0.9961, 0.9933, and 0.9612 for R^2 , adj- R^2 , and predicted R^2 , respectively (Table 16); however, according to the results of the analysis of variance, the quadratic model was the best model for predicting the sustainability index (*SI*) according to the relationship between the set of independent variables and the response of *SI*.

Based on Equation (27), the results showed that increasing the drying air temperature (*A*) and the thickness of the sample bed (*B*) during the drying process enhanced the sustainability index. The positive values of the interaction terms of the variables (*AB*) and their quadratic terms (A^2) and (B^2) showed that higher values of these variables increased this index. Consequently, according to Equation (27), the effect of the drying air temperature (*A*) on the sustainability index with a coefficient value (+0.0075) was much greater than the effect of the sample bed thickness (*B*) with a coefficient value (+0.0024). On the other hand, the drying air temperature parameter (A^2) had the most positive effect on the sustainability index with a coefficient of 0.0040 (Equation (27)), based on the combined effects.

$$SI = 0.0161 + 0.0075A + 0.0024B + 0.0014AB + 0.0040A^2 + 0.0005B^2 \quad (27)$$

SI describes the exergy supplied per unit of exergy loss in the drying chamber and is therefore inversely related to the exergy loss. A three-dimensional reaction surface curve and a two-dimensional contour of the changes for the sustainability index (*SI*) with the independent variables and their combined effects are shown in Figure 9a,b.

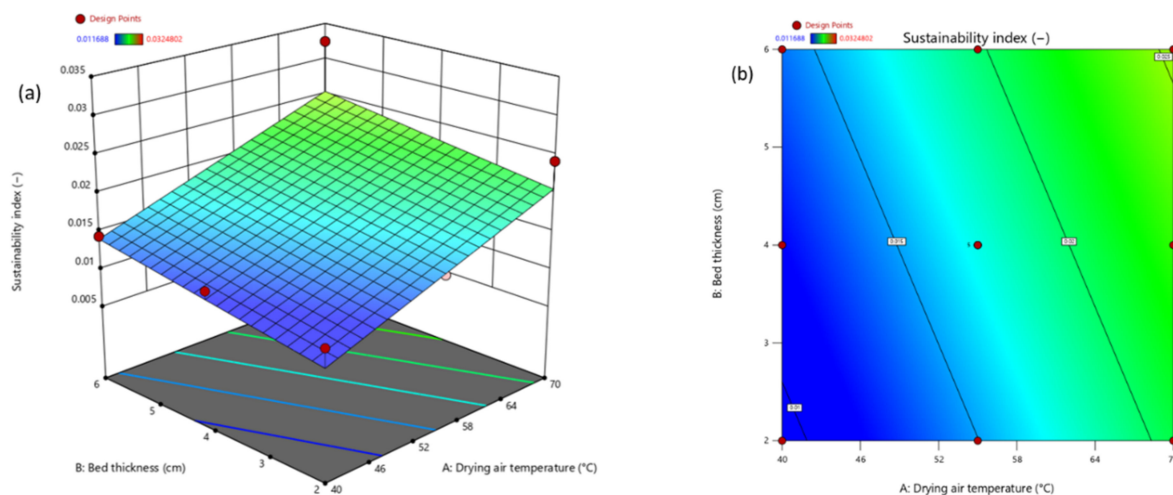


Figure 9. The effect of bed thickness and air temperature on the predicted response surface of sustainability index, (a) 3D response surface and (b) 2D contour plot.

From the surface plot, the minimum value of *SI* at an air temperature of 40 °C and a bed thickness of 2 cm was 0.0116, while the maximum value at an air temperature of 70 °C and a bed thickness of 6 cm was 0.0324. (Figure 9a,b); however, the results showed that the *SI* increased with an increasing drying air temperature and bed thickness. As a result, the *SI* was proportional to the drying air temperature and bed thickness. The higher the *SI* index, the lower the environmental impact and the higher the exergy efficiency. Similar results were obtained by Beigi, [59] for drying kiwifruit and Alhanif et al. [60] for drying papaya.

3.9. Optimization Analysis

In this section, the results of the optimization analysis and the desirability function of the independent parameters and responses for drying basil in a hybrid-solar dryer were evaluated. Figure 10 shows the desirability values of the drying air temperature, bed thickness, drying rate, energy utilization, energy utilization ratio, exergy efficiency and exergy loss rate, improvement potential rate, and sustainability index.

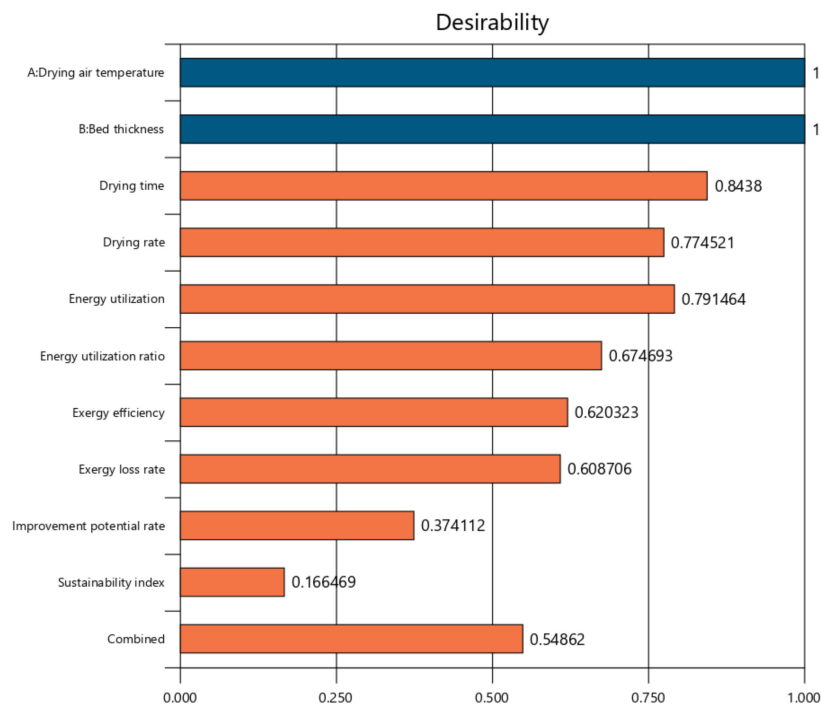


Figure 10. The values of individual desirability of input and response parameters for hybrid-solar dryer.

The RSM desirability function for the control factors (of drying air temperature and bed thickness) was 1, because they were set within the optimization range. Various responses (e.g., drying rate, energy utilization, energy utilization ratio, exergy efficiency, exergy loss rate, improvement potential rate, and sustainability index) were optimized to be tested at their minimum and maximum values. The desirability function values for the drying rate, energy utilization, energy utilization ratio, exergy efficiency, exergy loss rate, exergy improvement potential rate, and sustainability index were 0.774, 0.791, 0.674, 0.620, 0.608, 0.374, and 0.166, respectively (Figure 10). Finally, the combined suitability for this evaluation for drying the basil samples was 0.548. Table 17 presents the desired optimal values for all the independent and dependent optimization parameters using the desirability performance.

Table 17. Results of optimization by desirability function of RSM.

Parameters	<i>t</i> (°C)	<i>BT</i> (cm)	<i>Dr</i> (kg Water/kg Dry Matter min)	<i>EU</i> (kJ/s)	<i>EUR</i> (–)	<i>EX_{eff}</i> (%)	<i>EX_{loss}</i> (kJ/s)	<i>IP</i> (kJ/s)	<i>SI</i> (–)	Desirability
Optimum values	63.776	2.000	0.275	0.019	0.230	65.759	0.016	1.105	0.015	0.549

Optimal values of the control factors were obtained at a drying air temperature of 63.77 °C and a bed thickness of 2 cm. In addition, the optimum values for the drying rate, energy utilization, energy utilization ratio, exergy efficiency and losses, exergy improvement potential rate, and sustainability index parameters under these drying conditions were 0.275 (kg water/kg dry matter min), 0.019 kJ/s, 0.23, 65.75%, 0.016 kJ/s, 1.105 kJ/s, and 0.015, respectively, were obtained using the predicted response level method (Table 17).

Additionally, future research works could be directed to applying detailed conventional or even advanced exergoeconomic and exergoenvironmental assessments (e.g., integrating exergy and life cycle assessment (LCA) principles) to supplement our understanding from the monetary and environmental issues of the various drying systems in the food industry. It is expected that such comprehensive approaches can decrease the inefficiencies in thermodynamics, the total costs, and the total environmental impacts of food processing plants.

4. Conclusions

In this study, basil samples were dried from an initial moisture content to an equilibrium moisture content of 12% (d.b.) in a hybrid convective solar dryer. Energy and exergy analyses were accomplished by using the first and second laws of thermodynamics. The optimization process approach was undertaken based on the response surface method (RSM) and desirability function (DF) to find the optimal drying conditions for the drying air temperature and sample bed thickness at different surfaces on the drying rate, energy utilization, energy utilization ratio, exergy efficiency, exergy loss rate, exergy improvement potential rate, and sustainability index (*SI*). An analysis of variance showed that the drying air temperature based on the selected model had a greater effect on most responses than the sample bed thickness when carrying out the experiments. In the statistical regression analysis, it was found that the experimental data were properly fitted with a quadratic polynomial model RSM with a high coefficient of determination. In general, the most important thermodynamic property (exergy efficiency) increased with an increasing drying air temperature and bed thickness. Moreover, the results showed that the optimal conditions for the independent variables—obtained with an air temperature of 63.77 °C and bed thickness of 2 cm that optimized the responses of the drying rate (0.275 kg water/kg dry matter min), energy utilization (0.019 kJ/s), energy utilization ratio (0.230), exergy efficiency (65.75%), exergy loss rate (0.016 kJ/s), exergy improvement potential rate (1.105 kJ/s), and sustainability index (0.015)—were determined with a maximum desirability function of 0.548; therefore, the values of the IP showed that the exergy efficiency for the drying process of basil leaves can be increased. Moreover, the optimal values of these parameters obtained by RSM can help industrial engineers to provide efficient solutions for decreasing the exergy loss and improving the performance of industrial dryers, while decreasing the environmental impacts. As a result, the response surface method (RSM), with the developed models to predict all the responses and the optimization process of the desired parameters, was successful, which is an important technique to improve production in the food industry.

Author Contributions: Conceptualization, Z.P.; methodology, H.K.; software, I.G.; validation, Y.D., H.K.; formal analysis, N.A.O.; investigation, A.M.B.-M. and Z.P.; resources, J.D.M.; data curation, M.K. and M.S.; writing—original draft preparation, I.G., H.K. and Z.P.; writing—review and editing, A.M.B.-M., J.D.M., M.S., E.K. and S.S. All authors have read and agreed to the published version of the manuscript.

Funding: This research received no external funding.

Institutional Review Board Statement: Not applicable.

Informed Consent Statement: Not applicable.

Data Availability Statement: Data sharing is not applicable to this article.

Conflicts of Interest: The authors declare that they have no known competing financial interests or personal relationships that could have appeared to influence the work reported in this paper.

Nomenclature

Notations

MR	moisture ratio (dimensionless)
M	moisture content (% dry weight)
DR	drying rate
t	time (min)
\dot{E}_n	energy rate (kJ/s)
\dot{n}	mass flow rate (kg/s)
T	temperature ($^{\circ}\text{C}$)
P	atmospheric pressure (kPa)
A	area (m^2)
V	air velocity (m/s)
c_p	specific heat (kJ/kg $^{\circ}\text{C}$)
R	gas constant (8.3143 kJ/mol)
U	overall heat transfer coefficient (kW/m 2 $^{\circ}\text{C}$)
h	enthalpy (kJ/kg)
h_{fg}	latent heat of vaporization (kJ/kg)
EU	energy utilization (kJ/s)
EUR	energy utilization ratio (kJ/s)
EX	exergy rate (kJ/s)
Q	heat transfer (kJ/s)
IP	improvement potential rate (kJ/s)
SI	sustainability index
x	coded variable of model in RSM
RSM	response surface method
D	total desirability function
d	desirability function of each response in RSM

Greek letters

ρ	density (kg/m 3)
ψ_{ex}	exergy efficiency (%)
φ	relative humidity of air (%)
ω	humidity ratio (kg water/kg dry air)
t	time difference
α	coefficient term of RSM's model

Subscripts

∞	ambient
a	air
e	equilibrium
vs	saturated vapor
0	initial
L	heat loss
ij	numerator
in	inlet
L	loss
$w.b.$	wet basis
out	output
ph	physical
in	inlet air
out	outlet air
b	basil
fp	fresh product
dp	dried product
da	drying air
tp	triple point
evp	evaporation
hdb	hybrid dryer body
dc	drying chamber
p	pressure

References

1. Özcan, M.; Arslan, D.; Ünver, A. Effect of drying methods on the mineral content of basil (*Ocimum basilicum* L.). *J. Food Eng.* **2005**, *69*, 375–379. [\[CrossRef\]](#)
2. De Aquino Brito Lima-Corrêa, R.; dos Santos Andrade, M.; da Silva, M.F.d.G.F.; Freire, J.T.; Ferreira, M.d.C. Thin-layer and vibrofluidized drying of basil leaves (*Ocimum basilicum* L.): Analysis of drying homogeneity and influence of drying conditions on the composition of essential oil and leaf colour. *J. Appl. Res. Med. Arom. Plants* **2017**, *7*, 54–63. [\[CrossRef\]](#)
3. Parmar, M.R.; Kumpavat, M.T.; Doshi, J.S.; Kapdi, S.S. A comparative study on drying of basil leaves. *Agric. Eng. Int. CIGR J.* **2017**, *19*, 169–177.
4. El-Mesery, H.S.; El-Seesy, A.I.; Hu, Z.; Li, Y. Recent developments in solar drying technology of food and agricultural products: A review. *Renew. Sustain. Energy Rev.* **2022**, *157*, 112070. [\[CrossRef\]](#)
5. Karami, H.; Rasekh, M.; Darvishi, Y. Effect of temperature and air velocity on drying kinetics and organo essential oil extraction efficiency in a hybrid dryer. *Innov. Food Technol.* **2017**, *5*, 65–75.
6. Karami, H.; Rasekh, M.; Darvishi, Y.; Khaledi, R. Effect of Drying Temperature and Air Velocity on the Essential Oil Content of *Mentha aquatica* L. *J. Essent. Oil-Bear. Plants* **2017**, *20*, 1131–1136. [\[CrossRef\]](#)
7. Karami, H.; Lorestani, A.N.; Tahvilian, R. Assessment of kinetics, effective moisture diffusivity, specific energy consumption, and percentage of thyme oil extracted in a hybrid solar-electric dryer. *J. Food Proc. Eng.* **2021**, *44*, e13588. [\[CrossRef\]](#)
8. Erick César, L.-V.; Ana Lilia, C.-M.; Octavio, G.-V.; Orlando, S.S.; Alfredo, D.N. Energy and exergy analyses of a mixed-mode solar dryer of pear slices (*Pyrus communis* L.). *Energy* **2021**, *220*, 119740. [\[CrossRef\]](#)
9. Guiné, R.; Golpour, I.; Barroca, M.; Kaveh, M. Application of artificial neural networks (ANNs) modelling in drying technology of food products: A comprehensive survey. In *A Comprehensive Guide to Neural Network Modeling*; Nova Science Publishers, Inc.: Hauppauge, NY, USA, 2020.
10. Kaveh, M.; Golpour, I.; Gonçalves, J.C.; Ghafouri, S.; Guiné, R. Determination of drying kinetics, specific energy consumption, shrinkage, and colour properties of pomegranate arils submitted to microwave and convective drying. *Open Agric.* **2021**, *6*, 230–242. [\[CrossRef\]](#)
11. Golpour, I.; Kaveh, M.; Chayjan, R.; Guiné, R. Optimization of Infrared-convective Drying of White Mulberry Fruit Using Response Surface Methodology and Development of a Predictive Model through Artificial Neural Network. *Int. J. Fruit Sci.* **2020**, *20* (Suppl. 2), 1015–1035. [\[CrossRef\]](#)
12. Yogendrasasidhar, D.; Setty, Y.P. Drying kinetics, exergy and energy analyses of Kodo millet grains and Fenugreek seeds using wall heated fluidized bed dryer. *Energy* **2018**, *151*, 799–811. [\[CrossRef\]](#)
13. Beigi, M.; Torki, M.; Khoshnam, F.; Tohidi, M. Thermodynamic and environmental analyses for paddy drying in a semi-industrial dryer. *J. Therm. Anal. Calorim.* **2021**, *146*, 393–401. [\[CrossRef\]](#)
14. Afzali, F.; Darvishi, H.; Behrooz-Khazaei, N. Optimizing exergetic performance of a continuous conveyor infrared-hot air dryer with air recycling system. *Appl. Therm. Eng.* **2019**, *154*, 358–367. [\[CrossRef\]](#)
15. Erbay, Z.; Hepbasli, A. Application of conventional and advanced exergy analyses to evaluate the performance of a ground-source heat pump (GSHP) dryer used in food drying. *Energy Convers. Manag.* **2014**, *78*, 499–507. [\[CrossRef\]](#)
16. Gungor, A.; Tsatsaronis, G.; Gunerhan, H.; Hepbasli, A. Advanced exergoeconomic analysis of a gas engine heat pump (GEHP) for food drying processes. *Energy Convers. Manag.* **2015**, *91*, 132–139. [\[CrossRef\]](#)
17. Hernández, J.A.; Pavón, G.; García, M.A. Analytical solution of mass transfer equation considering shrinkage for modeling food-drying kinetics. *J. Food Eng.* **2000**, *45*, 1–10. [\[CrossRef\]](#)
18. Golpour, I.; Kaveh, M.; Chayjan, R.; Guiné, R. Energetic and exergetic analysis of a convective drier: A case study of potato drying process. *Open Agric.* **2020**, *5*, 563–572. [\[CrossRef\]](#)
19. Noshad, M.; Mohebbi, M.; Shahidi, F.; Ali Mortazavi, S. Multi-Objective Optimization of Osmotic-Ultrasonic Pretreatments and Hot-Air Drying of Quince Using Response Surface Methodology. *Food Bioprocess. Technol.* **2012**, *5*, 2098–2110. [\[CrossRef\]](#)
20. Soltani, A.; Azzouz, S.; Romdhana, H.; Goujot, D.; Elcafsi, M.A. Multi-response optimization of drying process parameters for *Laurus Nobilis*. *J. Appl. Res. Med. Aromat. Plants* **2021**, *22*, 100302. [\[CrossRef\]](#)
21. Taheri-Garavand, A.; Mumivand, H.; Fatahi, S.; Nasiri, A.; Omid, M. Modeling the kinetics of essential oil content and main constituents of mint (*Mentha aquatica* L.) leaves during thin-layer drying process using response surface methodology. *J. Food Process. Preserv.* **2021**, *45*, e15515. [\[CrossRef\]](#)
22. Domínguez-Niño, A.; Salgado-Sandoval, O.; López-Vidaña, E.C.; César-Munguía, A.L.; Pilatowsky-Figueroa, I.; García-Valladares, O. Influence of process variables on the drying kinetics and color properties of pear slices (*Pyrus communis*). *Color Res. Appl.* **2021**, *46*, 1128–1141. [\[CrossRef\]](#)
23. Obajemihi, O.I.; Olaoye, J.O.; Cheng, J.-H.; Ojediran, J.O.; Sun, D.-W. Optimization of process conditions for moisture ratio and effective moisture diffusivity of tomato during convective hot-air drying using response surface methodology. *J. Food Process. Preserv.* **2021**, *45*, e15287. [\[CrossRef\]](#)
24. Soodmand-Moghaddam, S.; Sharifi, M.; Zareiforoush, H. Investigation of fuel consumption and essential oil content in drying process of lemon verbena leaves using a continuous flow dryer equipped with a solar pre-heating system. *J. Clean. Prod.* **2019**, *233*, 1133–1145. [\[CrossRef\]](#)
25. Sasongko, S.B.; Hadiyanto, H.; Djaeni, M.; Perdanianti, A.M.; Utari, F.D. Effects of drying temperature and relative humidity on the quality of dried onion slice. *Heliyon* **2020**, *6*, e04338. [\[CrossRef\]](#)

26. Sadeghi, E.; Asl, A.; Movagharnejad, K. Optimization and quality evaluation of infrared-dried kiwifruit slices. *Food Sci. Nutr.* **2020**, *8*, 720–734. [[CrossRef](#)] [[PubMed](#)]
27. Majdi, H.; Esfahani, J.A.; Mohebbi, M. Optimization of convective drying by response surface methodology. *Comput. Electron. Agric.* **2019**, *156*, 574–584. [[CrossRef](#)]
28. Jafari, F.; Movagharnejad, K.; Sadeghi, E. Infrared drying effects on the quality of eggplant slices and process optimization using response surface methodology. *Food Chem.* **2020**, *333*, 127423. [[CrossRef](#)] [[PubMed](#)]
29. Zalazar-Garcia, D.; Román, M.C.; Fernandez, A.; Asensio, D.; Zhang, X.; Fabani, M.P.; Rodriguez, R.; Mazza, G. Exergy, energy, and sustainability assessments applied to RSM optimization of integrated convective air-drying with pretreatments to improve the nutritional quality of pumpkin seeds. *Sustain. Energy Technol. Assess.* **2022**, *49*, 101763. [[CrossRef](#)]
30. Karami, H.; Kaveh, M.; Mirzaee-Ghaleh, E.; Taghinezhad, E. Using PSO and GWO techniques for prediction some drying properties of tarragon (*Artemisia dracuncululus* L.). *J. Food Proc. Eng.* **2018**, *41*, e12921. [[CrossRef](#)]
31. Genc, S. *Exergetic Assessment in Dairy Industry*; IntechOpen: London, UK, 2018. [[CrossRef](#)]
32. Dincer, I.; Midilli, A.; Kucuk, H. *Progress in Exergy, Energy, and the Environment*; Springer: Berlin/Heidelberg, Germany, 2014; eBook; ISBN 978-3-319-04681-5.
33. Karami, H.; Kaveh, M.; Golpour, I.; Khalife, E.; Rusinek, R.; Dobrzański, B.; Gancarz, M. Thermodynamic Evaluation of the Forced Convective Hybrid-Solar Dryer during Drying Process of Rosemary (*Rosmarinus officinalis* L.) Leaves. *Energies* **2021**, *14*, 5835. [[CrossRef](#)]
34. Dincer, I.; Rosen, M.A. Energy, environment and sustainable development. *Appl. Energy* **1999**, *64*, 427–440. [[CrossRef](#)]
35. Khanali, M.; Aghbashlo, M.; Rafiee, S.; Jafari, A. Exergetic performance assessment of plug flow fluidised bed drying process of rough rice. *Int. J. Exergy* **2013**, *13*, 387–408. [[CrossRef](#)]
36. Gool, W. *Energy Policy: Fairy Tales and Factualities*; Springer: Berlin/Heidelberg, Germany, 1997; pp. 93–105.
37. Aghbashlo, M.; Kianmehr, M.H.; Arabhosseini, A. Energy and Exergy Analyses of Thin-Layer Drying of Potato Slices in a Semi-Industrial Continuous Band Dryer. *Drying Technol.* **2008**, *26*, 1501–1508. [[CrossRef](#)]
38. Beigi, M.; Tohidi, M.; Toriki-Harchegani, M. Exergetic analysis of deep-bed drying of rough rice in a convective dryer. *Energy* **2017**, *140*, 374–382. [[CrossRef](#)]
39. Nielsen, S. *Sustainable Development Indicators: An Exergy-Based Approach*; CRC Press: Boca Raton, FL, USA; Taylor and Francis Group: Milton Park, UK, 2020; 237p.
40. Li, S.; Chen, S.; Han, F.; Xu, Y.; Sun, H.; Ma, Z.; Chen, J.; Wu, W. Development and Optimization of Cold Plasma Pretreatment for Drying on Corn Kernels. *J. Food Sci.* **2019**, *84*, 2181–2189. [[CrossRef](#)]
41. Bensaha, A.; Benkouider, F.; Bekkouche, S.M.A.; Abdellaoui, A.; Chergui, T.; Benseddik, A. An Experimental Study of an Evacuated Tube Solar Collector Using the Response Surface Methodology (RSM). *Model. Meas. Control. B* **2019**, *88*, 106–111. [[CrossRef](#)]
42. Prashob, K.; Aniesrani Delfiya, D.S.; Murali, S.; Alfiya, P.V.; Samuel, M.P. Drying of shrimp using hot air-assisted continuous infrared drying system. *J. Food Process. Preserv.* **2022**. [[CrossRef](#)]
43. Horuz, E.; Bozkurt, H.; Karatas, H.; Maskan, M. Effects of hybrid (microwave-convectonal) and convectonal drying on drying kinetics, total phenolics, antioxidant capacity, vitamin C, color and rehydration capacity of sour cherries. *Food Chem.* **2017**, *230*, 295–305. [[CrossRef](#)] [[PubMed](#)]
44. Zheng, D.-J.; Cheng, Y.-Q.; Liu, H.-J.; Li, L.-T. Investigation of EHD-Enhanced Water Evaporation and a Novel Empirical Model. *Int. J. Food Eng.* **2011**, *7*. [[CrossRef](#)]
45. Moussaoui, H.; Bahammou, Y.; Tagnamas, Z.; Kouhila, M.; Lamharrar, A.; Idlimam, A. Application of solar drying on the apple peels using an indirect hybrid solar-electrical forced convection dryer. *Renew. Energy* **2021**, *168*, 131–140. [[CrossRef](#)]
46. Tagnamas, Z.; Kouhila, M.; Bahammou, Y.; Lamsyehe, H.; Haytem Moussaoui, H.; Idlimam, A.; Lamharrar, A. Drying kinetics and energy analysis of carob seeds (*Ceratonia siliqua* L.) convective solar drying. *J. Therm. Anal. Calorim.* **2022**, *147*, 2281–2291. [[CrossRef](#)]
47. Chen, X.; Du, W.; Liu, D. Response surface optimization of biocatalytic biodiesel production with acid oil. *Biochem. Eng. J.* **2008**, *40*, 423–429. [[CrossRef](#)]
48. Golpour, I.; Nejad, M.; Chayjan, R.; Nikbakht, A.M.; Guiné, R.; Dowlati, M. Investigating shrinkage and moisture diffusivity of melon seed in a microwave assisted thin layer fluidized bed dryer. *J. Food Meas. Charact.* **2017**, *11*, 1–11. [[CrossRef](#)]
49. Demirpolat, A.B.; Aydoğmuş, E.; Arslanoğlu, H. Drying behavior for *Ocimum basilicum* Lamiaceae with the new system: Exergy analysis and RSM modeling. *Biomass Convers. Biorefin.* **2022**, *12*, 515–526. [[CrossRef](#)]
50. Balasubramani, P.; Viswanathan, R.; Vairamani, M. Response surface optimisation of process variables for microencapsulation of garlic (*Allium sativum* L.) oleoresin by spray drying. *Biosyst. Eng.* **2013**, *114*, 205–213. [[CrossRef](#)]
51. Mehran, S.; Nikian, M.; Ghazi, M.; Zareiforoush, H.; Bagheri, I. Modeling and optimization of energy consumption and performance characteristics of a solar assisted fluidized bed dryer. *Energy Equipm. Syst.* **2020**, *8*, 401–425.
52. Das, H.; Mahanta, P.; Saikia, R.; Tamuly, P. Thermodynamic Analysis in Bubbling Fluidized Bed Dryers With Spiral and Cone Angles. *J. Therm. Sci. Eng.* **2021**, *13*, 1–24. [[CrossRef](#)]
53. Pattanayak, B.; Mohapatra, S.; Das, H. Energy and exergy analyses of paddy drying process in a vertical fluidised bed dryer. *Int. J. Exergy* **2019**, *28*, 113. [[CrossRef](#)]

54. Abano, E.; Ma, H.; Qu, W. Optimization of Drying Conditions for Quality Dried Tomato Slices Using Response Surface Methodology. *J. Food Process. Preserv.* **2013**, *38*, 996–1009. [[CrossRef](#)]
55. Suherman, S.; Susanto, E.E.; Zardani, A.W.; Dewi, N.H.R.; Hadiyanto, H. Energy–exergy analysis and mathematical modeling of cassava starch drying using a hybrid solar dryer. *Cogent Eng.* **2020**, *7*, 1771819. [[CrossRef](#)]
56. Kumar, D.; Prasad, S.; Murthy, G. Optimization of microwave-assisted hot air drying conditions of okra using response surface methodology. *J. Food Sci. Technol.* **2014**, *51*, 221–232. [[CrossRef](#)]
57. Nwakuba, N. Optimisation of energy consumption of a solar-electric dryer during hot air drying of tomato slices. *J. Agric. Eng.* **2019**, *50*, 150–158. [[CrossRef](#)]
58. Uzoma, S.; Nwakuba, N.; Anyaoha, K. Response surface optimization of convective air drying process in a hybrid PV/T solar dryer. *Turk. J. Agric. Eng. Res.* **2020**, *1*, 111–130.
59. Beigi, M. Moisture removal behavior and thermodynamic analysis of kiwifruit slices in convective tray dryer. *Lat. Am. Appl. Res.* **2022**, *52*, 119–126.
60. Alhanif, M.; Kumoro, A.C.; Wardhani, D.H. Mass transfer, energy utilization, physical and nutritional properties evaluations during drying of papaya (*Carica papaya* L.) seeds at low to moderate temperatures. *Arab. J. Sci. Eng.* **2022**, *47*, 6245–6267. [[CrossRef](#)]